Absolute measurement of the total ion-drag force on a single plasma-confined microparticle at the void edge under microgravity conditions

J. Beckers, D. J. M. Trienekens, and G. M. W. Kroesen

Eindhoven University of Technology, Department of Applied Physics, P.O. Box 513, 5600 MB, Eindhoven, the Netherlands

We present an absolute measurement of the total ion-drag force on one single microparticle at the edge of the dust free region in low pressure complex plasmas: the void. In order to do so, the particle confinement position was monitored as a function of the gas pressure for two particle sizes under normal gravity conditions and under microgravity conditions during parabolic flights. At the border of the void, the ion-drag force on a particle with a radius of 4.90 μm appeared to be $(3.6 \pm 0.3) \times 10^{-12}$ N.

I. INTRODUCTION

The ion-drag force—being the force exerted by streaming ions on dust particles in complex plasmas—is key in the formation of voids, dust free regions starting to develop from the center of the discharge. Voids have been recognized in both laboratory plasmas [1,2] and complex plasmas under microgravity conditions [3–5]. In addition to experiments, the formation of voids has been extensively studied theoretically and by means of computer simulations [6–8]. At the edges of such voids, force equilibrium on the dust particles applies. For instance, in experiments under microgravity conditions the void edge is at the position in the plasma where the outwards directed ion-drag force exerted on a particle is exactly compensated by the inwards electric force. In Ref. [9] Lipaev *et al.* demonstrated under microgravity conditions that it was indeed possible to close a void by reducing the ion-drag force with respect to the electrical force. In other work, researchers presented a method to determine particle charge, electron temperature, and ion density in a dusty plasma by monitoring the position and velocity of microparticles [10]. The force field inside the void was investigated by means of analyzing microparticles which are injected into the void by instabilities at the void boundary [11]. Although the ion-drag phenomenon is well understood, describing this force quantitively has been a continuous source for debate in literature for decades already [12,13]. Subject to these discussions are the questions on how to take into account the role of ion-neutral collisions [14,15] and how to treat shielding of the particle charge. For instance, Barnes *et al.* [16] and Kilgore *et al.* [17] assume that there is no interaction between the negatively charged microparticle and ions further away than one Debye length, while Khrapak *et al.* [18,19] consider scattering processes with impact parameters larger than the linearized Debye length as well. Another factor complicating the study of ion drag at the void edge is the fact that experiments on voids mean, per definition, that many dust particles are involved and that the ion drag on one particle is distorted by neighboring particles. Zafiu *et al.* [20] cleverly solved this issue by letting microparticles vertically fall through a discharge operated between vertically aligned electrodes and study horizontal particle motion initiated by the ratio between ion-drag and electrostatic forces F_i/F_E not being unity. Regardless of the choice of physical model, all experiments up to now need to use assumptions on plasma

parameters, such as ion velocity, local electric fields, charged particle densities, etc., to interpret the data.

In this Brief Report we present an absolute measurement of the ion-drag force on a single microparticle at the position where usually the induced void would have its edge.

II. METHOD

The results were obtained by performing measurements at a gas pressure which is chosen such that a single microparticle (particle 1 with mass m_{p1} and radius r_{p1}) under normal gravity conditions ($g = 1g_0$, with $g_0 = 9.81$ m/s^2) is vertically confined at the same positions z_{eq} as a larger microparticle (particle 2 with mass m_{p2} and radius r_{p2}) under microgravity conditions ($g = 0g_0$) during parabolic flights. The mentioned configurations are denoted with "Configuration 1" and "Configuration 2," respectively in Fig. 1.

On the particle in equilibrium position z_{eq} in configuration 1, the force balance consists of three dominant forces: the gravitational force $\vec{F}_{g1} = m_{p1}g_0$, the total ion-drag force $\vec{F}_{i1}(z_{eq})$, and the compensating electrostatic force $\vec{F}_{E1} = Q_{p1}(z_{eq})E_1(z_{eq})$. Here m_{p1}, $Q_{p1}(z_{eq})$, and $E_1(z_{eq})$ are the mass, the time-averaged local charge of particle 1, and the time-averaged local value of the sheath electric field, respectively. The force balance for configuration 1 at position z_{eq} yields

$$\vec{F}_{g1} + \vec{F}_{i1}(z_{eq}) = \vec{F}_{E1}(z_{eq}), \tag{1}$$

For configuration 2, the gravitational force is absent and, hence, the force balance—also at $z = z_{eq}$—is given by

$$\vec{F}_{i2}(z_{eq}) = \vec{F}_{E2}(z_{eq}). \tag{2}$$

In absence of gas flows (sealed vessel during experiments), the neutral drag force is zero. Furthermore, temperature gradients and laser intensity are sufficiently low that thermophoretic and laser-irradiation forces can safely be neglected (see also Ref. [21]). When realizing that at $z = z_{eq}$ the local electric field at the particle's equilibrium position is the same for both configurations, Eqs. (1) and (2) can be connected. Together with the assumptions that (i) the particle charge scales linearly with r_p [22] and (ii) the ion-drag force roughly scales with $r_p{}^2$ [18], the following relation between $\vec{F}_{i2}(z_{eq})$, the particle

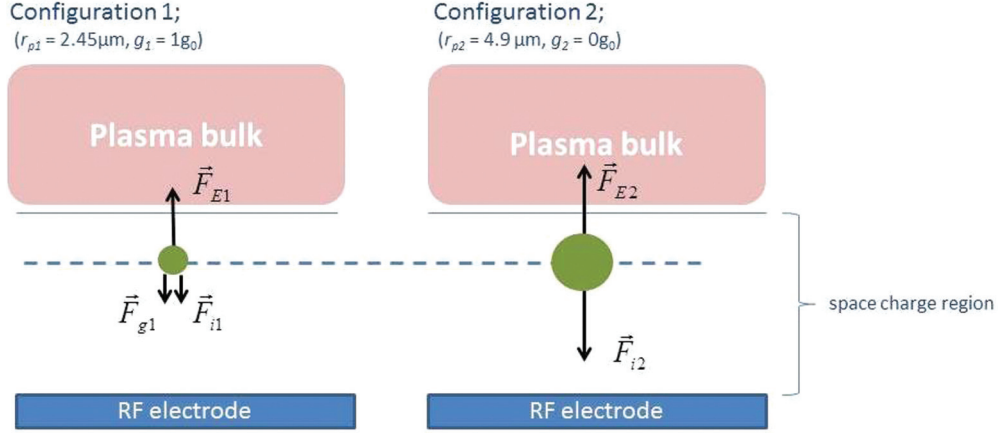FIG. 1. (Color online) Representation of a small particle ($r_{p1} = 2.45 \pm 0.05$ μm) under normal gravity conditions (Configuration 1) confined in the electric field in the plasma sheath at the same vertical position as a larger particle ($r_{p2} = 4.90 \pm 0.09$ μm) under microgravity conditions.

radii and $\vec{F}_{g1}$ is easily derived:

$$\vec{F}_{i2}(z_{eq}) = \left(\frac{r_{p1}}{r_{p2}} - \frac{r_{p1}^2}{r_{p2}^2} \right)^{-1} \vec{F}_{g1}. \quad (3)$$

III. EXPERIMENT

The experiments were performed in a sealed $200 \times 200 \times 200$ mm^3 aluminum vacuum chamber filled with argon gas at a certain set (but variable) pressure. A $\sim$5 W radio frequency (rf) driven (at 13.56 MHz) discharge was operated between two squared (70×70 mm^2) parallel plate electrodes aligned within the horizontal plane and vertically separated 40 mm. Microparticles of either 2.45 or 4.90 μm in radius were injected one by one by a home-built particle injector, after which they fell through a hole in the upper (grounded) electrode. Once in the discharge region, these particles gained negative charge and became confined within the electric field in the plasma sheath just above the rf powered lower electrode. A 1 mm deep indent in this electrode prevented the particles from horizontal loss. The geometrical size of this indent was chosen such that in the center, and at least a few millimeters around, the equipotential surface was horizontally flat; this has been verified by monitoring the equilibrium position of one full layer of monodisperse microparticles. The singly confined microparticle was illuminated by an expanded 532 nm diode laser beam while its vertical equilibrium position was monitored by a CCD camera behind a 532 nm interference filter with 20 ms time resolution. The apparent gravitational acceleration was measured in three perpendicular directions by an accelerometer with 20 ms time resolution as well. The vacuum chamber, together with the vacuum pump, gas- and power supplies, optics, and readout electronics, was mounted on a base plate, which was—for the microgravity experiments—mounted in the Novespace Airbus A300 with which parabolic flights were carried out. During these parabolic flights, the airplane originally flying at fixed height pulls up for about 20 s, inducing hypergravity conditions (at about $1.8g_0$). After this hypergravity phase, the airplane lowers its engine power such that it is just sufficient to overcome air friction. Hence, the airplane and all experiments in it are subject to free fall. This induces microgravity conditions for about 20 s after which the airplane has to pull up in order to prevent crashing.

It should be noted that the changes in apparent gravitational acceleration were sufficiently slow to allow the particle to adapt its equilibrium position instantaneously.

IV. RESULTS AND INTERPRETATION

Figure 2 gives the vertical confinement position of the particle with $r_p = 4.90$ μm as a function of time for three different gas pressures. As can be observed, during the hypergravity phase, the particles are pulled closer to the electrode. When via the second transition phase T the apparent gravitational acceleration is altered towards microgravity, the particle appears to be confined at positions closer to the plasma bulk, i.e., this is the position at which the ratio between the ion-drag and electrostatic forces F_i/F_E equals
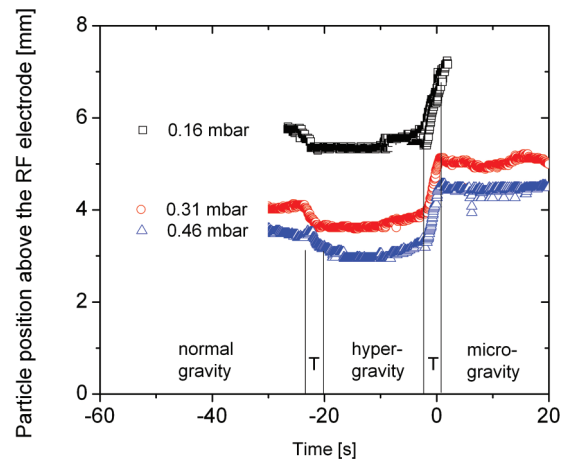

FIG. 2. (Color online) Particle position above the rf electrode of the $r_p = 4.90$ μm particle as a function of time during the hyper- and microgravity phases of a parabola for three values of the gas pressure.
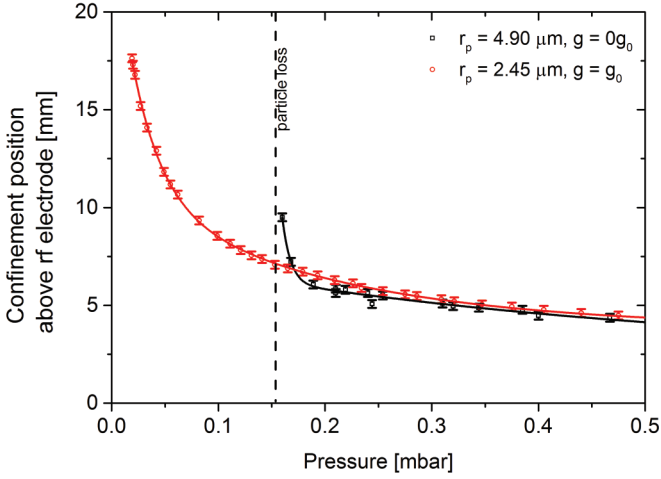
FIG. 3. (Color online) Particle position above the rf electrode as a function pressure for "configuration 1" (black squares) and "configuration 2" (red triangles) intersecting at $p = 0.18 \pm 0.01$ mbar.

unity, i.e., the traditional position of the void edge. As can be observed, at and below 0.16 mbar the microparticle is lost from the discharge under microgravity conditions. Since the particle would be vertically confined in the upper part of the discharge as well, the particle is thought to be lost horizontally by small horizontal accelerations in the airplane; at these high equilibrium positions, the horizontal confinement induced by the indent in the lower electrode is not effective anymore.

The vertical confinement positions of the $r_p = 4.90$ μm particle under microgravity conditions have been plotted as a function of the gas pressure in Fig. 3 together with the confinement position of the $r_p = 2.45$ μm particle under normal gravitational conditions in the laboratory. Indeed, these two profiles show intersection at 0.18 ± 0.01 mbar. At this intersection point Eq. (3) applies. At the corresponding position ($z = z_{eq} = 6.3 \pm 0.1$ mm) above the powered RF electrode, we find for the total ion-drag force on the $r_p = 4.90$ μm microparticle: $\vec{F}_{i2} = (3.6 \pm 0.3) \times 10^{-12}$ N. In this method, the error bar of 0.3×10^{-12} N is induced by the uncertainty in the radii of the particles used, influencing the uncertainty of the values of r_{p1}, r_{p2}, and $\vec{F}_{g1}$ in Eq. (3).

Although not used to determine $F_{i2}(z_{eq})$ we sum up some plasma parameters for this configuration in order to support future modeling efforts to reveal solutions to the fundamental questions left regarding the ion-drag force. For that we use the values found in Ref. [21] for exactly the same configuration and plasma settings at a pressure (0.20 mbar) very close to the intersection pressure found in this work: sheath width, 7.0 ± 0.5 mm; plasma potential, 32 ± 6 V; electrode bias potential, -82 ± 1 V; plasma density, $(7 \pm 2) \times 10^{14}$ m^{-3}; and electron temperature, 2.0 ± 0.5 eV.

Despite the fact that the found value for the total ion-drag force lays well within the range of ion-drag forces published in the literature [4,8], comparison of the results obtained here with that obtained in the literature is rather difficult. The reason for this is the fact that all measurements and

numerical simulations published so far have the necessity to make assumptions about the available models (e.g., shielding length, influence of collisions) and/or the need to measure or "guess" other plasma parameters such as the local ion velocity, electrical field, and plasma density.

V. THE MODEL'S SENSITIVITY TO THE USED ASSUMPTIONS

In our analysis, the error bar in the value of $F_{i2}(z_{eq})$ is determined by the uncertainties in r_{p1} and r_{p2}. Here we investigate the sensitivity of the obtained result against the two assumptions done. First, for the sensitivity with respect to the first assumption that the ion-drag force depends on r_p^2, we have determined the upper limit of the influence of the r_p dependence of the Coulomb logarithm taken into account in the orbital component of the ion-drag force [18,19]. Since the intersection point of the two curves in Fig. 3 is close to the transition from plasma sheath to plasma bulk [21], we have used for this estimate a directed ion velocity equal to the Bohm velocity and a Debye length as normally calculated in the plasma bulk. Assuming that 100% of the ion drag is delivered by the orbital-drag force (the collection component to the ion-drag force depends always on r_p^2), delivering the largest possible deviation from r_p^2 dependence of $F_{i2}(z_{eq})$, the influence is estimated at about 35% of the total value. Although at low ion velocities (close to the plasma bulk) the orbital component is large compared to the collection component, indeed, this deviation is an absolute overestimation. Second, we investigate the sensitivity of the result with respect to the second assumption that the particle charge depends linearly on r_p. Especially under conditions where collisions between streaming ions and neutrals become more important, these ions are caused to lose energy and may become trapped in the Debye cloud which electrostatically shields the negative charge on the particle. Once these ions are collected by the particle, this additional term in the ion current lowers the negative particle potential. From Ref. [23] we estimate that the maximum reduction in particle potential for the larger particle with respect to the smaller particle is about 10%. In turn, this effect may cause a deviation of the end result of less than 5%.

VI. CONCLUSION

In this Brief Report we have presented an absolute measurement of the total ion-drag force on one single microparticle at the traditional border of a void.

[1] H. Rothermel, T. Hagl, G. E. Morfill, M. H. Thoma, and H. M. Thomas, Phys. Rev. Lett. **89**, 175001 (2002).

[2] E. Thomas, B. M. Annaratone, G. E. Morfill, and H. Rothermel, Phys. Rev. E **66**, 016405 (2002).

[3] S. Ratynskaia *et al.*, Phys. Rev. Lett. **93**, 085001 (2004).

[4] V. E. Fortov *et al.*, Phys. Rep. **421**, 1 (2005).

[5] M. Wolter *et al.*, IEEE Trans. Plasma Sci. **35**, 266 (2007).

[6] J. Goree *et al.*, Phys. Rev. E **59**, 7055 (1999).

[7] V. N. Tsytovich, S. V. Vladimirov, G. E. Morfill, and J. Goree, Phys. Rev. E **63**, 056609 (2001).

[8] V. Land and W. J. Goedheer, New J. Phys. **8**, 8 (2006).

[9] A. M. Lipaev *et al.*, Phys. Rev. Lett. **98**, 265006 (2007).

[10] B. Liu *et al.*, Phys. Plasmas **17**, 053701 (2010).

[11] M. Kretschmer *et al.*, Phys. Rev. E **71**, 056401 (2005).

[12] S. A. Khrapak *et al.*, Phys. Plasmas **10**, 4579 (2003).

[13] C. Zafiu, A. Melzer, and A. Piel, Phys. Plasmas **10**, 4582 (2003).

[14] A. V. Ivlev, S. A. Khrapak, S. K. Zhdanov, G. E. Morfill, and G. Joyce, Phys. Rev. Lett. **92**, 205007 (2004).

[15] A. V. Ivlev *et al.*, Phys. Rev. E **71**, 016405 (2005).

[16] M. S. Barnes, J. H. Keller, J. C. Forster, J. A. O'Neill, and D. K. Coultas, Phys. Rev. Lett. **68**, 313 (1992).

[17] M. D. Kilgore *et al.*, J. Appl. Phys. **73**, 7195 (1993).

[18] S. A. Khrapak, A. V. Ivlev, G. E. Morfill, and H. M. Thomas, Phys. Rev. E **66**, 046414 (2002).

[19] S. A. Khrapak, A. V. Ivlev, G. E. Morfill, and S. K. Zhdanov, Phys. Rev. Lett. **90**, 225002 (2003).

[20] C. Zafiu, A. Melzer, and A. Piel, Phys. Plasmas **10**, 1278 (2003).

[21] J. Beckers *et al.*, Phys. Rev. Lett. **106**, 115002 (2011).

[22] A. Bouchoule (editor), *Dusty Plasmas: Physics, Chemistry, and Technological Impact in Plasma Processing* (Wiley & Sons, New York, 1999).

[23] Z. Sternovsky, M. Lampe, and S. Robertson, IEEE Trans. Plasma Sci. **32**, 632 (2004).